AIAA JOURNAL
Vol. 44, No. 2, February 2006

Increasing Allowable Flight Loads by Improved Structural Modeling

Erdem Acar,* Raphael T. Haftka,† Bhavani V. Sankar,‡ and Xueshi Qiu§
University of Florida, Gainesville, Florida 32611

The tradeoffs of allowable flight loads and safety of aerospace structures via deterministic and probabilistic design methodologies are analyzed. The methodologies are illustrated by performing allowable flight load calculation of a sandwich panel used in aerospace structures. The effect of using a more accurate prediction technique for interfacial fracture toughness that combines interfacial fracture toughness with mode mixity instead of using the traditional model that disregards mode mixity is explored. It was found that by utilizing this more accurate model with the change in *B*-basis properties, the deterministic approach allows a 13.1% increase in the allowable flight load and a reduction of probability of failure by a factor of five. The probabilistic approach allows a 26.5% increase in allowable flight load, while maintaining the original probability of failure.

Nomenclature

C	=	capacity of structure, for example, yield stress
e^A, e^{MM}	=	errors in fracture toughness assessment corresponding to traditional (averaging) method and method with mode mixity, respectively
e_C, e_R	=	error factors for C and R, respectively
e_{rms}	=	rms error
G	=	strain energy release rate
K_1, K_2	=	mode 1 and 2 stress intensity factors, respectively
p, $p_{\max}$	=	load and critical load, respectively
p_{allow}	=	allowable flight load
R	=	response of structure, for example, stress
R^2_{adj}	=	adjusted coefficient of multiple determination
S_F	=	safety factor
VAR_C, VAR_R	=	variabilities of C and R, respectively
ψ	=	mode-mixity angle

I. Introduction

STRUCTURAL design of aerospace structures is still performed with a deterministic design philosophy. Researchers are constantly improving the accuracy of structural analysis and failure prediction. This improvement in accuracy reduces uncertainty in aircraft design and can, therefore, be used to enhance safety. However, because the record of structural safety in civilian transport aircraft is very good, it makes sense to ask how to translate the reduced uncertainty to increased flight loads or weight reduction if safety is to be maintained at a specified level. The term allowable flight load refers here to the maximum allowable load that can be carried by the structure for a specific failure mode. Currently, there is no accepted way to translate the improvements in accuracy to weight savings or increased allowable flight loads. The objective of this paper is to take the first step in this direction by utilizing probabilistic design methodology. Haftka[1] describes how the work of Li et al.[2] and Arbocz and Starnes[3] to model variability in the buckling of circular cylinders inspired work in his research group on using variability control to reduce the weight of composite liquid hydrogen tanks. Qu et al.[4] showed that for a fixed probability of failure, small reductions in variability can be translated to substantial weight savings. Here we seek to investigate the potential of improved structural modeling.

Some commercial aircraft that entered service in 1970s or 1980s are expected to reach their design service life soon. However, because researchers are constantly improving the accuracy of structural analysis and failure prediction, the maximum allowable flight loads of those aircraft can be recalculated to utilize the full potential of their structures. Motivated by this goal, we consider a given aerospace structure that is already designed, and we aim to re-calculate the allowable flight load of the structure due to improved analysis. We expect that for some designs, lower allowable loads will be predicted by the improved analysis, whereas for others higher allowable flight loads will be predicted. However, because improved models reduce uncertainty, we may expect an average increase of the allowable flight loads over all designs. An important focus of the paper is to show that modeling error can masquerade as observed variability, which can be reduced (or even eliminated) by a better understanding of the physical phenomenon.

In this paper, we chose a sandwich panel as an example because the improved model was developed by one of the authors, and we had good access to the details of the experiments and computations. Sandwich structures are used in aerospace vehicles due to their low areal density and high stiffness. Debonding of the core from the face sheet is a common failure mode in sandwich construction, and the interfacial fracture is traditionally characterized by a single fracture toughness parameter. However, in reality, the fracture toughness is a function of the relative amount of mode 2 to mode 1 (mode mixity) acting on the interface.[5] The stiffness of sandwich structures depends very much on the integrity of the face sheet/core bonding. Even a small disbond can significantly reduce the load carrying capacity, especially when the structure is under compressive loads.[6,7] Grau et al.[8] measured the interfacial fracture toughness as a function of mode mixity to characterize the propagation of the disbond between the face sheet and the core. They performed asymmetric double cantilever beam fracture tests to determine the interfacial fracture toughness of the sandwich composite and then demonstrated its application in predicting the performance of a sandwich structure containing a disbond. The use of mode-mixity-dependent fracture toughness led to improvement in the accuracy of failure prediction of the debonded structure. In this paper, we perform probabilistic

Presented as Paper 2005-2167 at the AIAA/ASME/ASCE/AHS/ASC 46th Structures, Structural Dynamics, and Materials Conference, Austin, TX, 18–21 April 2005; received 22 May 2005; revision received 4 October 2005; accepted for publication 4 October 2005. Copyright © 2005 by the American Institute of Aeronautics and Astronautics, Inc. All rights reserved. Copies of this paper may be made for personal or internal use, on condition that the copier pay the $10.00 per-copy fee to the Copyright Clearance Center, Inc., 222 Rosewood Drive, Danvers, MA 01923; include the code 0001-1452/06 $10.00 in correspondence with the CCC.

*Research Assistant, Department of Mechanical and Aerospace Engineering; eacar@ufl.edu. Student Member AIAA.

†Distinguished Professor, Department of Mechanical and Aerospace Engineering; haftka@ufl.edu. Fellow AIAA.

‡Ebaugh Professor, Department of Mechanical and Aerospace Engineering; sankar@ufl.edu. Associate Fellow AIAA.

§Visiting Researcher, Department of Mechanical and Aerospace Engineering; currently Senior Engineer, Structural Mechanics Department, South West United Machinery Corporation, Chengdu 610041, People's Republic of China.

analysis of the debonded sandwich structure analyzed by the deterministic approach by Grau et al.[8] to explore a possible increase in the allowable flight load of the structure.

The following section discusses the design of a sandwich structure used as an illustration. Section III presents the analysis of structural uncertainties (error and variability) with the primary perspective of how to control uncertainty. Discussion of the calculation of B-basis properties and allowable flight load calculation for sandwich structures by deterministic design are given in Sec. IV. In Sec. V, the assessment of the probability of failure of sandwich structures is presented. In Sec. VI, the tradeoffs of accuracy and allowable flight load via probabilistic design are discussed. Finally, concluding remarks are given in Sec. VII.

II. Structural Analysis of Sandwich Structure

Sandwich panels are susceptible to debonding of the face sheet from the core. This is similar to the phenomenon of delamination in laminated composites. Disbonds can develop due to poor manufacturing or during service, for example, due to foreign object impact damage. The evaluation of damage and prediction of residual strength and stiffness of debonded sandwich panels is critical because the disbonds can grow in an unstable manner and can lead to catastrophic failure. The stiffness of sandwich structures depends very much on the integrity of the face sheet/core bonding. Even a small disbond can significantly reduce the load carrying capacity, when the structure is under compressive loads[6,7] because the debonded face sheet can buckle and create conditions at the crack tip that are conducive for unstable propagation of the disbond. This problem has become very significant after the historic failure of the X-33 vehicle fuel tank made up of sandwich panels of polymer matrix composite face sheets and a honeycomb core.

Fracture at the interface between dissimilar materials is a critical phenomenon in many multimaterial systems including sandwich construction. Traditionally, in engineering practice, the interfacial fracture was characterized by a single fracture toughness parameter obtained by averaging the interfacial fracture toughness, hereinafter termed average G_c or G_c^A, obtained for some number of K_1 and K_2 combinations, where K_1 and K_2 are the mode 1 and mode 2 stress intensity factors, respectively. Later studies have indicated,[5] that for these multimaterial systems, the interfacial fracture is a strong function of the relative amount of mode 2 to mode 1 acting on the interface, hereinafter termed G_c with mode mixity or G_c^{MM}. The criterion for initiation of crack advance at the interface can be stated as

$$G = G_c(\psi), \qquad \psi = \tan^{-1}(K_2/K_1) \tag{1}$$

where G_c is the interfacial fracture toughness, which depends on the mode-mixity angle ψ. In bimaterial fracture, K_1 and K_2 are the real and imaginary parts of the complex stress intensity factor K. The toughness of interface $G_c(\psi)$ can be thought of as an effective surface energy that depends on the mode of loading.

Grau et al.[8] analyzed a debonded sandwich panel and determined the maximum internal gas pressure in the core before the disbond could propagate. They used interfacial fracture mechanics concepts to analyze this problem. The main premise here is that the crack will propagate when the energy release rate equals the fracture toughness for the core/face-sheet interface. The load and boundary conditions for the model problem are shown in Fig. 1. Note that due to symmetry only one-half of the structure is modeled.

The maximum allowable pressure for a given disbond length is calculated from the energy release rate G_0 for a unit applied pressure. The energy release rate G is proportional to the square of the applied load or

$$G = G_0 p^2 \tag{2}$$

where p is the applied pressure. This failure assessment is a good approximation within the limits of a linear analysis. We assume that the epistemic uncertainty related to this failure function is negligible compared to the uncertainty in fracture toughness. The critical pressure $p_{\max}$ can be obtained using

$$p_{\max} = \sqrt{G_c/G_0} \tag{3}$$

where G_c is the interfacial fracture toughness of the sandwich material system obtained from testing.

Grau[9] conducted asymmetric double cantilever beam tests to determine the interfacial fracture toughness of the sandwich composite. [The face-sheet material was A50TF266 S6 class E, fiber designation T800HB-12K-40B, matrix 3631, and the core sheet material was Euro-Composites aramid fiber-type honeycomb.] Grau et al.[8] performed finite element analyses to compute the mode-mixity angle corresponding to designs tested in experiments. The average interfacial fracture toughness prediction and the fracture toughness in terms of mode-mixity angle based on their work are shown in Fig. 2. The continuous line denotes average G_c (G_c^A) and the dashed line denotes a linear least square to fit to G_c, G_c^{MM}, as a function of mode-mixity angle. The linear fit has $R^2_{\mathrm{adj}} = 0.473$ and $e_{\mathrm{rms}} = 121.6$ N/m.

As shown in Fig. 2, a simple way of determining the interfacial fracture toughness parameter is to perform fracture toughness tests for different core thickness, face-sheet thickness, and crack length combinations, which correspond to different mode-mixity values, and to take the average fracture toughness value. However, as seen from Fig. 2, the critical energy release rate is assessed better as a function of mode mixity. Grau et al.[8] represent the critical energy

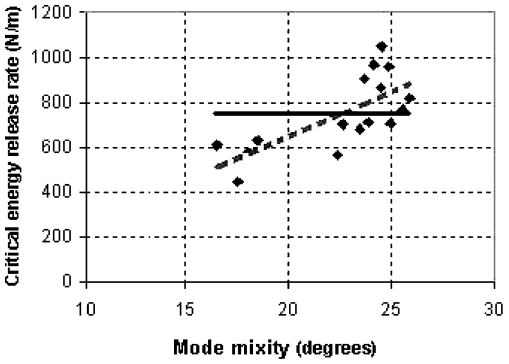

Fig. 2 Critical energy release rate as function of mode mixity.

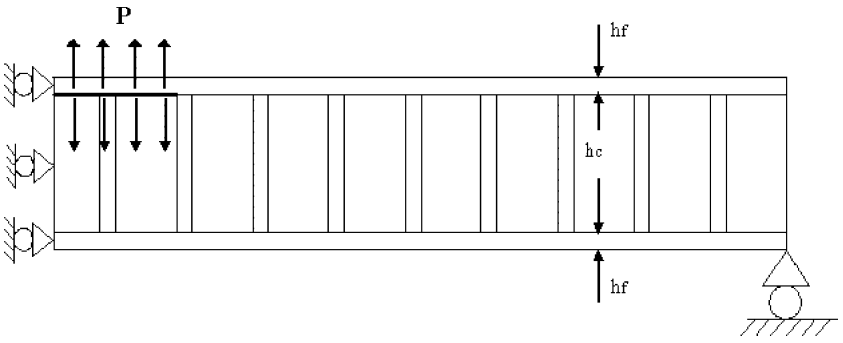

Fig. 1 Model of face-sheet/core debonding in one-dimensional sandwich panel with pressure load.

Table 1 Uncertainty classification

Type	Spread	Cause	Remedy
Error (mostly epistemic)	Departure of average fleet of aerospace structure model, for example, Boeing 737-400, from ideal	Errors in predicting structural failure, construction errors, deliberate changes	Testing and simulation to improve math model and solution
Variability (aleatory)	Departure of individual structure from fleet level average	Variability in tooling, manufacturing process, and flying environment	Improving tooling and construction, applying quality control

release rate as a linear function of the mode mixity, which they calculate from finite element analysis, that improves the accuracy of estimate of G_c.

From Fig. 2, we note that without the mode-mixity model, G_c would exhibit huge scatter, from 443 to 1047 N/m. The mode-mixity model reduces the scatter because instead of a constant, G_c is now predicted to vary from 513 to 875 N/m. That is, the simplicity of the average G_c model causes error in that model to masquerade as variability. For instance, the model of constant gravity acceleration constant g will lead to a scatter when measured in different cities, partially due to the difference in altitude. A model that takes altitude into account will show less scatter around the computed value of g. The uncertainty reduction, in turn, can be used to increase the safety or the effectiveness of the structure.

III. Analysis of Error and Variability

A good review of different sources of uncertainty in engineering modeling and simulations is provided by Oberkampf et al.[10,11] As in previous works,[12,13] we simplify the classification as shown in Table 1 to distinguish between uncertainties that apply equally to the entire fleet of a structural component and uncertainties that vary for an individual structure. In addition, this simple classification makes it easy to analyze the effects of uncertainty control. The uncertainties that affect the entire fleet are called errors here. They reflect inaccurate modeling of physical phenomena, errors in structural analysis, errors in load calculations, or use of materials and tooling in construction that are different from those specified by the designer. The variability (aleatory uncertainty) reflects variability in material properties, geometry, or loading between different copies of the same structure.

For the sake of simplicity, we assume that with mode mixity there are no remaining errors in the predicted value of G_c for a given mode-mixity angle calculated from finite element analysis. Adding an estimate of the remaining error can be easily accommodated by the analysis to follow. However, we assume that the scatter of G_c around mode-mixity-dependent G_c represents variability. The experimental values given in Table 2 are the mean values of the fracture toughness measured through five experiments by Grau et al.[8] for each mode mixity. We assume that the use of these mean values eliminates most of the measurement variability and leaves out only the material variability. In contrast, the scatter around the average G_c represents a combined error and variability.

The deviations of experimentally measured fracture toughness values from the two fits d^A and d^{MM}, the deviations from the constant fit and from the linear fit (Fig. 2), given in Table 2 are calculated from

$$d^A = G_c^{\exp} - G_c^A, \qquad d^{\mathrm{MM}} = G_c^{\exp} - G_c^{\mathrm{MM}} \tag{4}$$

Each row of Table 2 corresponds to a different specimen. Each specimen has a different core thickness, face-sheet thickness, and crack length, thus, having a different mode-mixity angle (calculated through finite element analysis). The sixth column of Table 2 lists the deviations of G_c values obtained through experiments from their average values. These deviations combine variability and error. Errors are due to neglecting the effect of mode mixity in G_c. (We assume that these are the only errors, so that d^{MM} represents only variability.)

The approximate cumulative distribution function (CDF) for the variability is obtained by using ARENA software.[14] The distribution parameters and goodness-of-fit statistics for the distributions are as follows. For variability d^{MM}, ARENA found the best distribution to be the normal distribution with a mean value of zero and a standard deviation of 113.8. For obtaining goodness-of-fit statistics, chi-square and Kolmogorov–Smirnov tests are the commonly used. For our case, the number of data points is low; hence, the chi-square test does not provide reliable statistics; therefore, ARENA uses the Kolmogorov–Smirnov test to decide if a sample comes from a population with a specific distribution. The p value of the Kolmogorov–Smirnov test is greater than 0.15. For total uncertainty d^A, ARENA found the best distribution to be the normal distribution with a mean value of zero and a standard deviation of 162.2.

Table 2 Deviations between measured and fitted values of average G_c and G_c with mode mixity for different designs

Specimen	ψ, deg	$G_c^{\exp}$, N/m	G_c^A,[a] N/m	G_c^{MM},[b] N/m	d^A,[c] N/m	d^{MM},[c] N/m
1	16.52	609.4	746.6	513.2	−137.1	96.2
2	17.53	443.1	746.6	552.2	−303.5	−109.1
3	18.05	577.9	746.6	572.3	−168.7	5.6
4	18.50	628.7	746.6	589.7	−117.9	39.0
5	22.39	565.7	746.6	739.5	−180.9	−173.8
6	23.89	711.0	746.6	797.1	−35.6	−86.1
7	24.50	863.4	746.6	820.6	116.8	42.8
8	24.89	956.2	746.6	835.9	209.6	120.3
9	23.48	679.5	746.6	781.4	−67.1	−101.9
10	24.98	707.5	746.6	839.3	−39.1	−131.7
11	25.55	767.1	746.6	861.1	20.5	−94.1
12	25.90	817.8	746.6	874.8	71.3	−56.9
13	22.65	702.3	746.6	749.3	−44.3	−47.1
14	23.69	903.7	746.6	789.5	157.1	114.1
15	24.15	964.9	746.6	807.2	218.4	157.7
16	24.54	1047.3	746.6	822.3	300.7	224.9
Std. dev.	——	162.2	0	115.6	162.2	113.8

[a]Average fracture toughness.
[b]Mode-mixity dependent fracture toughness.
[c]Deviation of experimental values from constant fit or from linear fit.

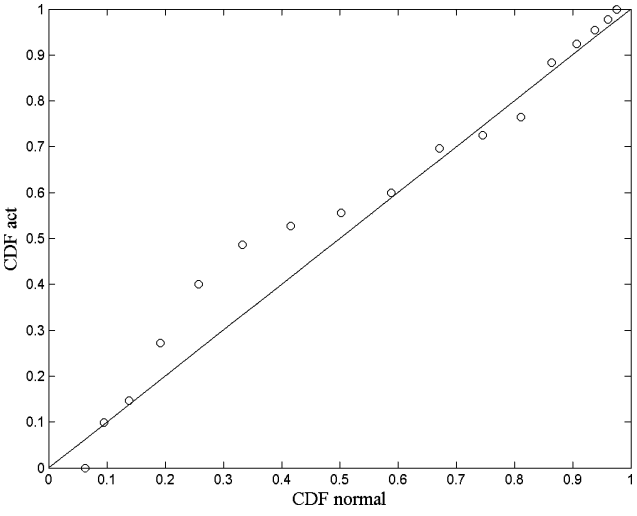

Fig. 3 Comparison of actual and fitted cumulative distribution functions of variability, d^{MM}, of G_c.

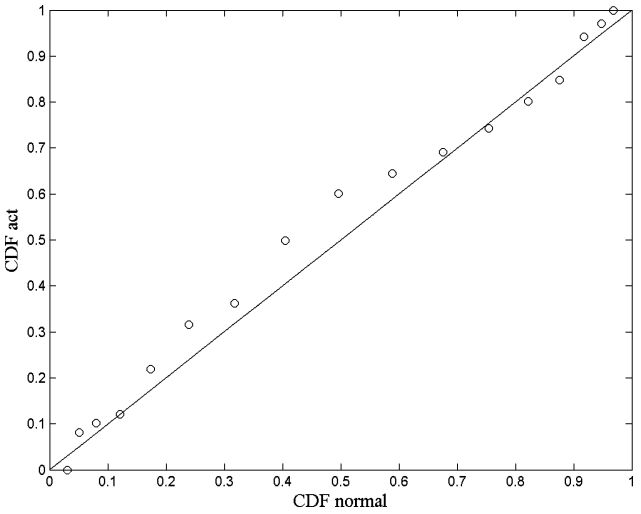

Fig. 4 Comparison of actual and fitted cumulative distribution functions of total uncertainty (error and variability, d^A) of G_c.

The p value for the Kolmogorov–Smirnov test is again greater than 0.15. The corresponding p value is a measure for goodness of the fit. Larger p values indicate better fits,[14] with p values less than about 0.05 indicating poor fit.

Figures 3 and 4 show the comparison of the actual and fitted CDFs of the variability (Fig. 3) and the total uncertainty (Fig. 4) of the average fracture toughness, respectively. In Figs. 3 and 4, the x axis represents the fitted CDF, whereas the y axis represents the actual CDF. If the fits were exact, they would follow the linear lines shown in Figs. 3 and 4. We see in Figs. 3 and 4 that the deviations from the linear lines are not high; hence, the fitted distributions are acceptable. Fitting is performed using ARENA software. The Kolmogorov–Smirnov test p value is greater than 0.15.

In addition to variability in G_c predictions, there is also variability in the pressure p. We assume that the maximum lifetime loading p follows lognormal distribution with mean value of p_{allow} and coefficient of variation of 10%.

IV. Deterministic Design and *B*-Basis Value Calculations

In deterministic design, the only use of probabilistic (or statistical) information is via conservative material properties, which are determined by the statistical analysis of material tests. Federal Aviation Administration (FAA) regulations (FAR-25.613) state that the conservative material properties are characterized as A-basis and B-basis material property values. A-basis values are used when there is a single failure path in the structure, whereas the B-basis values are used when there are multiple failure paths in the structure. Detailed information on these values is provided in Chapter 8 of Ref. 15.

In this paper, we use B-basis G_c, which is defined as the value exceeded by 90% of the population (of material batches) with 95% confidence. This is given by

$$B\text{ basis} = \mu - \sigma k_B \tag{5}$$

where μ is the mean, σ is the standard deviation, and k_B is the tolerance coefficient needed to achieve the 90% setoff and the 95% confidence. If infinitely many material characterization tests were carried out, there would be no issue of confidence, and for normal distribution, 90% of the population will be exceeded by $k_B = z_{0.1} = \Phi(0.1) = 1.282$, where Φ is the CDF of the standard normal distribution. With a finite sample of N tests, this is adjusted as

$$k_B = \left(z_{0.1} + \sqrt{z_{0.1}^2 - ab}\right)\Big/ a$$

$$a = 1 - z_{0.05}^2\Big/2(N-1), \qquad b = z_{0.1}^2 - z_{0.05}^2\Big/N \tag{6}$$

Table 3 Mean and *B*-basis values of fracture toughness of 13 designs analyzed

Design	Mode mixity, deg	$(G_c)^A_{\text{mean}}$, N/m	$(G_c)^{\text{MM}}_{\text{mean}}$, N/m	$(G_c)^A_{B\text{-basis}}$,[a] N/m	$(G_c)^{\text{MM}}_{B\text{-basis}}$, N/m
1	16.24	638.8	498.4	308.8	266.9
2	17.15	638.8	529.0	308.8	297.5
3	18.95	638.8	589.6	308.8	358.1
4	21.08	638.8	661.3	308.8	429.8
5	22.27	638.8	701.3	308.8	469.8
6	18.32	638.8	568.4	308.8	336.9
7	20.18	638.8	630.9	308.8	399.4
8	22.27	638.8	701.4	308.8	469.9
9	23.41	638.8	739.7	308.8	508.2
10	18.28	638.8	567.1	308.8	335.6
11	19.86	638.8	620.2	308.8	388.7
13	21.57	638.8	708.6	308.8	477.1

[a] B-basis values are calculated assuming that the improvements in accuracy affect the B-basis values.

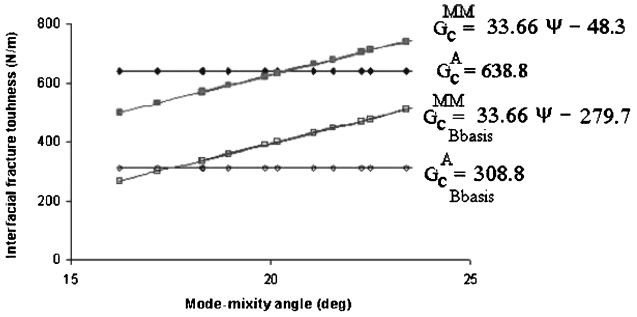

Fig. 5 Fitted least-square lines for fracture toughness and derived *B*-basis allowables.

where $z_{0.1} = \Phi(0.1)$ is the critical value of normal distribution that is exceeded with a probability of 10%.

Grau et al.[8] used the fracture toughness values obtained from experiments to calculate the predicted failure load of a debonded sandwich structure shown earlier in Fig. 2. They used different core thickness, face-sheet thickness, and crack length combinations and compared the predicted failure load of the structures designed via the use of average G_c and mode-mixity-dependent G_c. In their failure load calculation, Grau et al.[8] used the mean values for the fracture toughness, and they did not use a safety factor.

In this paper, we use B-basis values for fracture toughness and a safety factor of 1.4 for loading to assess the allowable flight load of the same sandwich designs used by Grau et al.[8] To calculate B-basis values, we use the standard deviations for fracture toughness given in Table 2. The mean values and the corresponding B-basis values of the fracture toughness for the 13 designs given in the example in Ref. 8 are given in Table 3.

Even though the scatter around the average G_c is combination of error and variability, for deterministic design following FAA regulations it is treated as variability. The reduced standard deviation of the mode-mixity-dependent G_c then allows increasing the allowable B basis. Figure 5 shows the fitted and B-basis values of the two approaches.

While calculating the B-basis values for fracture toughness given in Table 3, we use $N = 16$, which increases k_B to 2.035. Recall that the standard deviations σ of designs are obtained in the preceding section. For example, for the first design the mean value is 638.8. The corresponding B-basis value is calculated as $638.8 - 2.035 \times 162.2 = 308.8$.

After obtaining the B-basis values in Table 3, we compute the allowable flight load p_{allow} by deterministic design philosophy. As noted earlier, in addition to the use of B-basis material properties, a safety factor of 1.4 is also used for loads. Hence, Eq. (3) is modified to calculate the allowable flight loads for 13 different designs as

$$p_{\text{allow}} = (1/1.4)\sqrt{(G_c)_{B\text{-basis}}/G_0} \tag{7}$$

Table 4 Allowable flight load of failure of sandwich panels designed using deterministic approach

Design	Allowable flight load		
	$(p_{\text{allow}})^{A}$,[a] kPa	$(p_{\text{allow}})^{\text{MM}}$,[b] kPa	$\%\Delta p$
1	51.2	47.6	−7.0
2	267.0	262.0	−1.9
3	158.6	170.8	7.7
4	77.1	90.9	18.0
5	45.2	55.8	22.3
6	247.2	258.2	4.4
7	154.1	175.3	13.7
8	73.1	90.2	23.4
9	42.8	54.8	28.3
10	247.2	257.7	4.2
11	146.2	164.1	12.2
12	70.1	84.3	20.2
13	40.8	50.7	24.3
Average			13.1

[a]Use of average fracture toughness of experiments.
[b]Use of mode-mixity-dependent fracture toughness.

The calculated p_{allow} values corresponding to the use of G_c^A and G_c^{MM} are given in Table 4. The last column of Table 4 shows the percent change in the allowable flight load by using G_c^{MM} instead of G_c^A. We see that allowable flight load is increased by 13.1% on average by using the mode-mixity-based B-basis properties. This is the improvement in allowable flight load using a deterministic approach. As shown in the next section, this increase in allowable flight load is accompanied by a reduction in probability of failure, so that the additional gains may be realized by using a probabilistic approach.

V. Assessment of Probability of Failure

The probability of failure of a structural component can be expressed in terms of its structural response R and its capacity C corresponding to that response by

$$P_f = \text{Prob}\,(C \le R) \tag{8}$$

For the sandwich structure analyzed here, the response $R = G$ is the energy release rate [Eq. (2)], and the capacity $C = G_c$ is the interfacial fracture toughness. G depends on structural dimensions through G_0 [Eq. (2)]. Both response G and the capacity G_c have variability that needs to be included in the calculation of the probability of failure. We assume that the variability in G is mainly due to the variability in load p rather than G_0. Besides variability, there exist errors in assessing G and G_c, for example, errors in load G_0 and material property calculations.

The general equation for probability of failure given in Eq. (8) can be expressed in this problem as

$$P_f = \text{Prob}\left(G_c \le G_0 p^2\right) \tag{9}$$

Then, the probability of failure can be written in functional form as

$$P_f = P_f\left(\bar{G}_c, e_{G_c}, \text{VAR}_{G_c}, p_{\text{allow}}, \text{VAR}_P, G_0\right) \tag{10}$$

where $\bar{G}_c$ is the mean value of G_c, e_{G_c} is the error in G_c predictions that we reduce by using mode-mixity-dependent G_c instead of average G_c, VAR_{G_c} is the variability in G_c, p_{allow} is the allowable flight load (or mean value of the loading p), VAR_P is the variability in p, and G_0 is the strain energy release rate corresponding to unit pressure that we assume to be deterministic. Because the limit-state function for this problem, $g = G_c - G_0 p^2$, is a simple function with only two random variables, we easily calculate the probability of failure by analytical means as follows.

The probability distribution function (PDF) of a function Z of two random variables X and Y, $Z = h(X, Y)$, can be calculated as (Ang and Tang,[16] p. 170)

$$f_Z(z) = \int_{-\infty}^{\infty} f_{X,Y}(x, y)\left|\frac{\partial x}{\partial z}\right| \mathrm{d}y \tag{11}$$

where $f_{X,Y}(x, y)$ is the joint PDF of x and y. We can write the limit-state function for the sandwich panel problem as

$$g = G_c - G_0 p^2 \tag{12}$$

Therefore, to calculate the PDF of g from Eq. (11), we replace Z with g, X with G_c, and Y with p. We also have $G_c = g + G_0 p^2$, so that $|\partial x/\partial z| = |\partial G_c/\partial g| = 1$. After these substitutions and noting that p only takes positive values, we get from Eq. (11)

$$f_G(g) = \int_0^{\infty} f_{G_c,p}\left(g + G_0 p^2, p\right) \mathrm{d}p \tag{13}$$

Here we assume that G_C and p are statistically independent; hence, the joint distribution in Eq. (13) is calculated as

$$f_{G_c,p}(g + G_0 p^2, p) = f_{G_c}\left(g + G_0 p^2\right) f_p(p) \tag{14}$$

Then, the CDF of g is calculated as

$$F_G(g') = \int_{-\infty}^{g} f_G(g')\,\mathrm{d}g' \tag{15}$$

which allows us to compute the probability of failure simply as $P_f = F_G(0)$.

Table 5 shows the probabilities of failure corresponding to deterministic allowable flight loads. We observe that in addition to the 13.1% average increase in allowable flight load, the average probability of failure was reduced by about a factor of five.

Notice that the probabilities of failure given in Table 5 are high. These probabilities of failure correspond to component failure probabilities. The probability of the actual structure will be much smaller due to the redundancy in the structure. For example, if we define the failure of the structure as simultaneous failures of two components having a correlation coefficient (of probability of failure) of 0.5, then component probabilities of failure 1.869×10^{-3} and 0.369×10^{-3} given in the last row of Table 5 correspond to system probabilities of failure 1.280×10^{-4} and 0.139×10^{-4}, respectively.

Table 5 Corresponding probabilities of failure of sandwich panels designed using deterministic approach[a]

Designs	Probability of failure	
	P_f^{A}[b] (10^{-3})	P_f^{MM}[c] (10^{-3})
1	1.869	1.064
2	1.869	0.762
3	1.869	0.407
4	1.869	0.211
5	1.869	0.153
6	1.869	0.504
7	1.869	0.275
8	1.869	0.153
9	1.869	0.117
10	1.869	0.511
11	1.869	0.304
12	1.869	0.184
13	1.869	0.145
Average	1.869	0.369

[a]B-basis values are calculated considering that the improvements in accuracy affect the B-basis values (adjusted B-basis values).
[b]Use of average fracture toughness of experiments.
[c]Use of mode-mixity-dependent fracture toughness.

Table 6 Allowable flight loads of sandwich panels calculated via probabilistic approach

	$P_f = 1.869 \times 10^{-3}$		
Design	$(p_{\text{allow}})^{A}$,[a] kPa	$(p_{\text{allow}})^{\text{MM}}$,[b] kPa	$\%\Delta p$
1	51.2	50.5	−1.3
2	266.9	283.9	6.4
3	158.6	190.1	19.9
4	77.1	102.6	33.1
5	45.2	63.2	39.8
6	247.3	285.2	15.3
7	154.2	196.9	27.7
8	73.1	102.3	39.9
9	42.8	62.4	45.8
10	247.3	284.4	15.0
11	146.2	184.0	25.8
12	70.1	95.4	36.1
13	40.8	57.6	41.1
Average			26.5

[a]Use of average fracture toughness of experiments.
[b]Use of mode-mixity-dependent fracture toughness.

VI. Effects of Improved Model on Allowable Flight Load via Probabilistic Design

As seen from Eq. (10), there are four distinct ways to increase the allowable flight load of a structure: 1) Use a different material to increase $\bar{G}_c$. 2) Develop more accurate solutions that reduce e_{G_c} (such as the use of mode-mixity-dependent G_c instead of average G_c). 3) Improve quality control and manufacturing processes to reduce variability VAR_{G_c} or employ measures to reduce VAR_P. 4) Use a heavier design to reduce G_0. For a structure that is already built, only option 2 is available.

The preceding section showed how reductions in variability can increase allowable flight load using deterministic design. For probabilistic design, the mode-mixity approach is treated as an accuracy improvement, and we calculate its effect on the safe allowable flight load.

For a target probability of failure $(P_f)_{\text{target}}$, the allowable flight load can be calculated from

$$P_f = P_f\left(\bar{G}_c, e_{G_c}, \text{VAR}_{G_c}, p_{\text{allow}}, \text{VAR}_P, G_0\right) = (P_f)_{\text{target}} \quad (16)$$

Thus, given the target probability of failure, the allowable flight loads corresponding to different error factors on fracture toughness e_{G_c} can be calculated from Eq. (17),

$$P_f\left(e_{G_{c1}}, p_{\text{allow1}}\right) = P_f\left(e_{G_{c2}}, p_{\text{allow2}}\right) = (P_f)_{\text{target}} \quad (17)$$

For the present calculation, the target probability of failure is taken to be 1.869×10^{-3}, which is the probability of failure with the deterministic allowable flight load using the average G_c. (See Table 5.) Table 6 shows the comparison of allowable flight load for the average G_c and mode-mixity-dependent G_c approaches in the case of probabilistic design. We see in Table 6 that by fixing the probability of failure rather than adjusting the B-basis properties, the average allowable flight load can be increased by 26.5%. Note, however, that for some structures the improved analysis may indicate a small reduction in allowable flight loads. With the deterministic approach, this is applied to designs 1 and 2 (Table 4), whereas with the probabilistic approach, only design 1 suffers a small load reduction.

VII. Conclusions

The effect of an improved model for fracture toughness on allowable flight load was investigated using both deterministic and probabilistic design methodologies. For deterministic allowable flight load calculation, the improved model reduces scatter and allows an increase in the fracture toughness allowable calculated by B-basis properties, whereas for probabilistic allowable flight load calculation, the reduced error is incorporated into the calculation of probability of failure. We find that the deterministic approach leads to a 13.1% increase on average in the allowable flight load and reduction of the probability of failure by a factor of five. The use of B-basis properties in the deterministic design does not permit translating the full potential of improved modeling to increase allowable flight loads. In contrast, the probabilistic approach allows a 26.5% increase on average in the allowable flight load, while still maintaining the original probability of failure.

Acknowledgments

This research is supported by the NASA Constellation University Institute Program (formerly URETI) Grant NCC3-994 to the Institute for Future Space Transport at the University of Florida. The Cognizant Program Manager is Claudia Mayer at NASA John H. Glenn Research Center at Lewis Field.

References

[1]Haftka, R. T., "Reflections on Jim Starnes' Technical Contributions," AIAA Paper 2005-1872, April 2005.

[2]Li, Y., Elishakoff, I., Starnes, J. H., Jr., and Bushnell, D., "Effect of the Thickness Variation and Initial Imperfection on Buckling of Composite Cylindrical Shells: Asymptotic Analysis and Numerical Results by BOSOR4 and PANDA2," *International Journal of Solids and Structures*, Vol. 34, No. 28, 1997, pp. 3755–3767.

[3]Arbocz, J., and Starnes, J. H., "Hierarchical High-Fidelity Analysis Methodology for Buckling Critical Structures," *Journal of Aerospace Engineering*, Vol. 18, No. 3, 2005, pp. 168–178.

[4]Qu, X., Haftka, R. T., Venkataraman, S., and Johnson, T. F., "Deterministic and Reliability-Based Optimization of Composite Laminates for Cryogenic Environments," *AIAA Journal*, Vol. 41, No. 10, 2003, pp. 2029–2036.

[5]Suo, Z., "Singularities, Interfaces and Cracks in Dissimilar Anisotropic Media," *Proceedings of the Royal Society of London, Series A: Mathematical and Physical Sciences*, Vol. A427, 1999, pp. 331–358.

[6]Avery, J. L., and Sankar, B. V., "Compressive Failure of Sandwich Beams with Debonded Face-Sheets," *Journal of Composite Materials*, Vol. 34, No. 14, 2000, pp. 1176–1199.

[7]Sankar, B. V., and Narayanan, M., "Finite Element Analysis of Debonded Sandwich Beams Under Axial Compression," *Journal of Sandwich Structures and Materials*, Vol. 3, No. 3, 2001, pp. 197–219.

[8]Grau, D. L., Qiu, X., and Sankar, B. V., "Relation Between Interfacial Fracture Toughness and Mode-Mixity in Honeycomb Core Sandwich Composites," *Journal of Sandwich Structures and Materials* (to be published).

[9]Grau, D., "Relating Interfacial Fracture Toughness to Core Thickness in Honeycomb-Core Sandwich Composites," M.S. Thesis, Mechanical and Aerospace Engineering Dept., Univ. of Florida, Gainesville, FL, Dec. 2003.

[10]Oberkampf, W. L., DeLand, S. M., Rutherford, B. M., Diegert, K. V., and Alvin, K. F., "A New Methodology for the Estimation of Total Uncertainty in Computational Simulation," AIAA Paper 99-1612, April 1999.

[11]Oberkampf, W. L., Deland, S. M., Rutherford, B. M., Diegert, K. V., and Alvin, K. F., "Error and Total Uncertainty in Modeling and Simulation," *Reliability Engineering and System Safety*, Vol. 75, 2002, pp. 333–357.

[12]Acar, E., Kale, A., Haftka, R. T., and Stroud, W. J., "Why Airplanes Are so Safe Structurally? Effect of Various Safety Measures," *Journal of Aircraft* (to be published).

[13]Acar, E., Kale, A., and Haftka, R. T., "Effects of Error, Variability, Testing and Safety Factors on Aircraft Safety," *Proceedings of the NSF Workshop on Reliable Engineering Computing*, 2004, pp. 103–118.

[14]Kelton, W. D., Sadowski, R. P., and Sadowski, D. A., "Simulations with Arena," WCB McGraw–Hill, Boston, 1998, pp. 132–139.

[15]"Statistical Methods," *Composite Materials Handbook*, MIL-HDBK-17, Vol. 1, American Society for Testing and Materials, Baltimore, MD, 2002, Chap. 8.

[16]Ang, A. H., and Tang, W. H., *Probability Concepts in Engineering Planning and Design, Volume I: Basic Principles*, Wiley, New York, 1975, p. 170.

A. Palazotto
Associate Editor